

BOOK OF TUTORIALS AND ABSTRACTS



European Microbeam Analysis Society

EMAS 2009

11th

EUROPEAN WORKSHOP

on

MODERN DEVELOPMENTS

AND

APPLICATIONS

IN

MICROBEAM ANALYSIS

10 to 14 May 2009

at the

Hotel Spa Faltom

Gdynia/Rumia, Gdansk, Poland

Organized in collaboration with
Silesian University of Technology
Polish Society for Microscopy (PTMi)
Polish Academy of Sciences:
Committee of Materials Science, Institute of Physics,
Institute of Materials Science and Metallurgy



75 YEARS OF KOSSEL PATTERNS - PAST AND FUTURE

Enrico Langer and S. Däbritz

Dresden University of Technology, Institute for Solid State Physics
Helmholtz Strasse 10, DE-01062 Dresden, Germany

Dr. Enrico Langer is an academic assistant and fully involved in the training and management responsibilities of the Institute for Solid State Physics at the Dresden University of Technology. He obtained his diploma in physics in the field of Kossel X-ray micro-diffraction and his Ph.D. in physics at the same institution with the thesis “Effect of crystal defects on Kossel and pseudo-Kossel X-ray interferences” in 2005. He is currently working towards his qualification as a university lecturer (Habilitation). Dr. Langer leads a group, whose research focuses on developing new methods using these special X-ray micro-diffraction techniques in combination with electron backscattered diffraction, especially for the characterisation of crystal defects in the scanning electron microscope. Recently, the first X-ray fluorescence excited Kossel diffraction patterns in the SEM could be presented using a polycapillary lens. In the meantime, he has become an authority in the field of Kossel interferences. He has been a member of EMAS since 1998. Dr. Langer is vice-chairman of the Microprobe Group of the German Physical Society. Frequently as the main author, he has published more than 20 refereed scientific articles in international journals as well as over 30 contributions to national and international conferences in proceedings.

1. ABSTRACT

In the year of events 2009 of this EMAS conference the discovery of X-ray interferences from lattice sources is celebrating its 75th anniversary. This effect was discovered by Walther Kossel, named after him, in the city of Gdansk. Hereby, the X-ray source is located within the crystal itself and interferences (lattice source interferences) appear whose evaluation leads to significant physical material parameters. Therefore, lattice constants with a precision of 10^{-5} can be determined non-destructively in the micro-range. Both, the lattice parameter and the local crystal structure, can be ascertained at low and high temperatures, which make an important contribution to the investigations of crystallographic lattice transformations and especially to the characterisation of superconductors. Incipient with the first Kossel investigations on copper single-crystals in Gdansk up to computer simulated results on metals, intermetallic compounds, Cu-Sn phases (e.g., $\text{Cu}_{41}\text{Sn}_{11}$), as well as on complex materials, such as BaTiO_3 , correspondingly running diffusion processes in microelectrical contacts the Kossel technique, complemented by the wide angle method and the electron backscattering diffraction (EBSD), provides comprehensive answers to current questions of research. The contribution in hand gives selected application examples from different fields. Moreover, the most important development steps of the Kossel interferences or rather the physical phenomena and developments during the past years with a close connection to it should be briefly reviewed here.

2. INTRODUCTION

2.1. Chapters in Kossel's life in Heidelberg, Munich, Kiel, Gdansk and Tübingen

Walther Kossel, born on January 4, 1888 in Berlin, was an outstanding physicist, both as an experimenter and as a theorist (Fig. 1). His father, Albrecht Kossel, a professor of physiology in Heidelberg, was awarded the Nobel Prize for medicine in 1910. Walther Kossel studied physics at the University of Heidelberg and completed his doctorate there under the Nobel Prize winner Philipp Lenard. In an inspiring scientific sphere at the University of Munich, which was marked by the Nobel laureates Conrad Wilhelm Röntgen, Arnold Sommerfeld and Max von Laue, he explained, among other things, the X-ray spectra with the help of the Bohr model of an atom and developed the theory of the electron shell structure of the atoms. In 1921 he became a full professor of theoretical physics at the University of Kiel. There, he continued his work in Munich on X-ray spectra and valence forces. In 1928 he put forward a theory of crystal growth (Kossel crystal) together with I.N. Stranski.

In 1932 Walther Kossel moved to Danzig, now Gdansk, where he was appointed a chair at the Technische Hochschule Danzig (now the Gdansk University of Technology), but this time as a professor of experimental physics. The excellent experimental opportunities at Gdansk were not only of benefit to the evidence of X-ray interferences from lattice sources (Kossel pattern),



Figure 1. Walther Kossel, 1888 - 1956 (from [1]).

but also led, together with his pupil G. Möllenstedt in 1938, to the development of the convergent beam electron diffraction method (CBED, Kossel-Möllenstedt pattern). After 1947, he became a professor in Tübingen, attaining further results in the field of electron diffraction.

2.2. The discovery of Kossel interferences in Gdansk

Walther Kossel predicted the interference of the characteristic X-rays within the crystal, in which the self-radiation is excited, the so-called interferences from lattice sources, in 1924 [2]. This had initially erroneously been supposed by M. von Laue, W. Friedrich und P. Knipping in 1912 to be the cause of the interference phenomena of X-ray radiation. Ten years later in 1934, this X-ray diffraction effect was proved, for the first time by means of electron excitation on a copper single-crystal in Gdansk (Danzig at that time) by W. Kossel, V. Loeck und H. Voges [3]. Fig. 2 shows a historical sketch Kossel's on the left, schematically, of the experimental setup used. The cathode beam (1 mm diaphragm diameter) hits the copper single-crystal sphere, and the patterns are observed in back reflection by means of X-ray film [3]. As can be seen in the historical Fig. 2, in the thermal spot of the crystal the self-radiation is emitted with increased intensity according to the Bragg equation in those directions, which are defined through the Bragg angle, θ_B . Fig. 3 shows one of the first historical Kossel patterns of copper with the reflection calculation belonging to it. In the strong background the curves with increased intensity, which are called Kossel lines in Walther Kossel's honour, can be seen. Finally, in a time line (Fig. 4) the essential stages from the beginning of the Kossel technique up to today are pointed out.

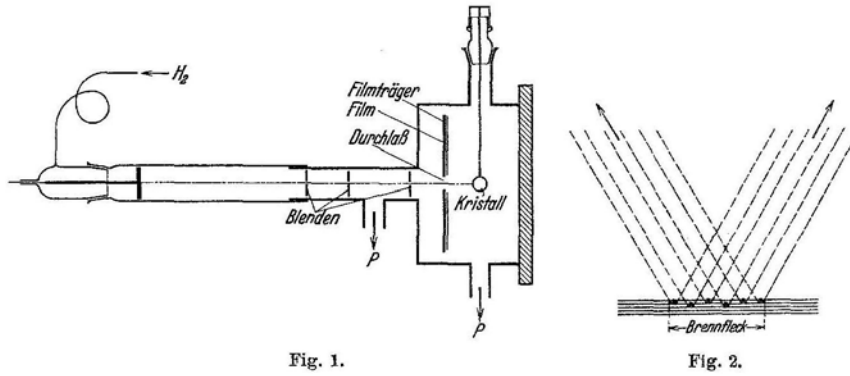


Figure 2. Historic schematic sketch of the used experimental setup in 1934 (historic figures 1 and 2 from [3]).

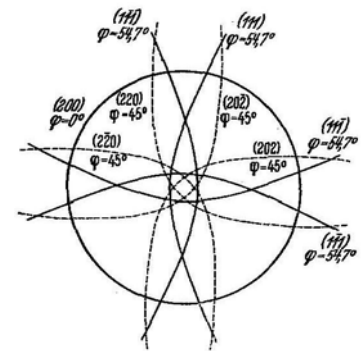
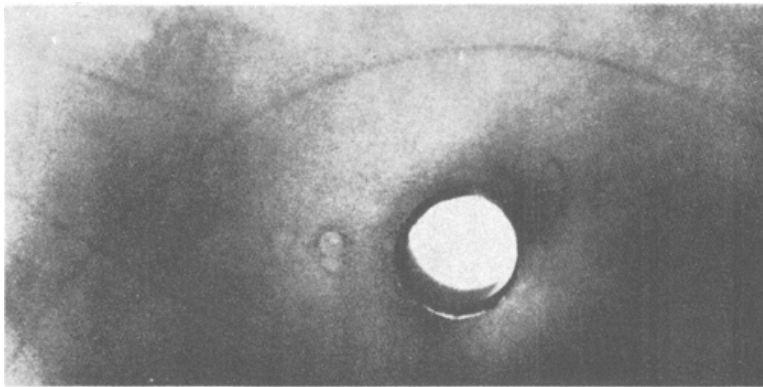


Fig. 6 a. Würfelpol.

Figure 3. First historic X-ray lattice source interference or Kossel pattern of Cu with reflection calculation belonging to it by W. Kossel, V. Loeck and H. Voges observed in Gdansk in 1934 at the Institute for Physics of the nowadays Gdansk University of Technology (historic figures 3 and 6a from [3]).

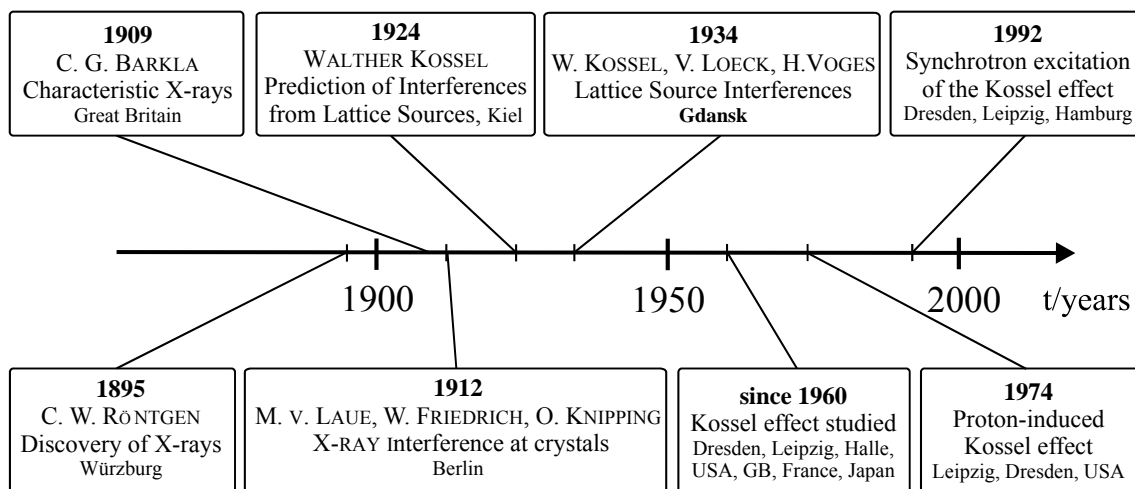


Figure 4. Time line of discoveries and investigations.

2.3. The principle of the Kossel effect in detail

For the *Kossel effect*, the emission of characteristic X-ray radiation within the investigated crystalline or quasi-crystalline volume is used [4]. The excitation is executed with electron, ion, proton X-ray and synchrotron radiation, respectively. The lattice atoms excited by means of the beam are starting points of the spherical waves of characteristic X-rays, which are diffracted at all neighbouring lattice points. These again become origins of spherical propagating scattering waves. The three-dimensional crystal lattice leads to the complex interference phenomena, and the resulting wave field has to be dealt within the scope of the dynamic theory of X-ray interferences [5].

In the background blackening outside the crystal a family of pure dark and bright cones appear and also such cones with a *bright-dark fine structure* or dark-bright structure, i.e., a bright border on the short wavy (convex) face of the lateral surface of the cone follows a dark part and vice versa. The crystal structure defines the geometrical positions and intensities of the so-called Kossel cones. Then the diffraction patterns show a system of curves, which can be understood as lines of intersections of the Kossel cones with the detection plane, i.e., conical sections, curves of the second order.

Diffraction geometry

The geometry of the Kossel lines, but by no means their fine structure of the lines, can be illustrated if the X-ray diffraction is interpreted as the reflection of the divergent incident rays on the family of the lattice planes of the crystal (Fig. 5). Since $\sin\theta_B \leq 1$ must be valid, the Bragg equation $2d^{\text{sample}} \sin\theta_B = n \lambda^{\text{sample}}$ can only be fulfilled for the Kossel method if the wavelength λ^{sample} of one of the excited self-radiations of the atoms is small, when compared with the lattice constants. Therefore, pure Mg, Al, and Si, do not show any Kossel lines. Here, the pseudo-Kossel method can overcome the problem by choosing the suitable target material (see Fig. 14).

3. DIFFERENT EXCITATION METHODS FOR THE KOSSEL EFFECT

3.1. Electron excitation

As already discussed, the Kossel effect was first proved by electron excitation in Gdansk (Danzig) in 1934 [3]. This is also the most widespread method today since it is applicable in the scanning electron microscope (see Fig. 5) or electron probe microanalyzer, attaining a high lateral resolution of up to 1 μm . At a probe current of 0.1 μA and an acceleration voltage of 20 kV the exposure time is only a few minutes.

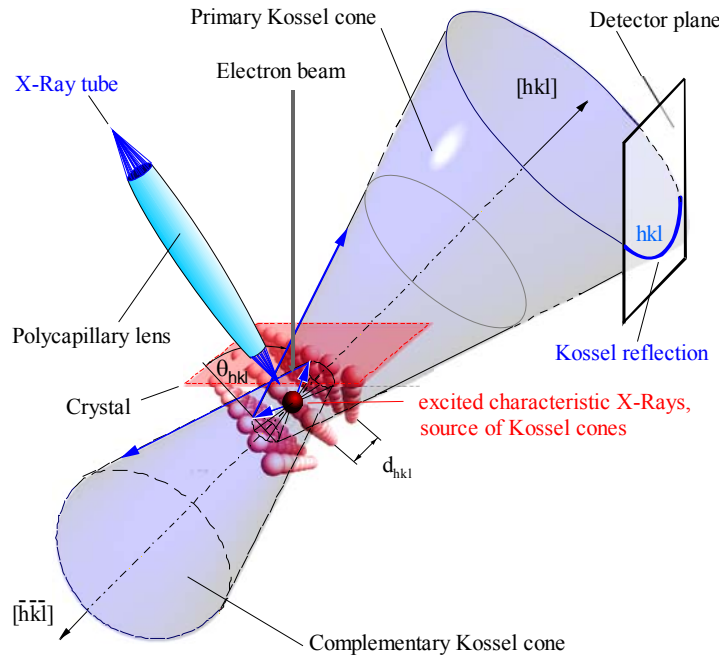


Figure 5. Basic principle of the Kossel effect with different excitation methods (electrons and X-rays using a polycapillary lens) as used in Dresden presently.

3.2. X-ray excitation

Not long afterwards Borrmann, an assistant in Kossel's laboratory successfully carried out his idea of an excitation by X-rays [6]. So far, for the application of conventional X-ray tubes, long integration times (24 h) conditional on the slight attainable intensities were required. As our investigations, which are discussed in section 5, show, this can, nowadays, be markedly improved by the use of polycapillary lenses (Fig. 5).

3.3. Proton or ion beam excitation

The 1 MeV proton-induced Kossel effect were first proved on GaP semiconductor single-crystals (reflection (111), P-K α -radiation) by V. Geist and R. Flaggmeyer [7] in 1974. Shortly thereafter, J. B. Roberto *et al.* [8] and H.-J. Ullrich *et al.* [9], independent of each other, observed proton-induced Kossel patterns on metal crystals ($E_p = 2$ MeV on Cu and $E_p = 5.6$ MeV on Fe as well as Ni, resp.).

3.4. Synchrotron radiation excitation

In 1992, H.-J. Ullrich *et al.* [10] detected Kossel interferences by polychromatic synchrotron radiation excitation. In comparison with an X-ray tube the many times higher intensity leads to substantially shorter exposure times of several seconds. Ch. Schetelich *et al.* [11] used monochromatic synchrotron radiation with the advantage of a selective excitation of one characteristic radiation.

4. APPLICATION EXAMPLES

Table 1 shows an overview of the most important information which can be determined by lattice source interferences (Kossel method) in comparison with the pseudo-Kossel diffraction (PKD) as well as electron backscattering diffraction (EBSD) [12]. Some application fields of the *Kossel technique* shall be presented in detail in this contribution.

Table 1. Comparison and application ranges of the three different methods [12].

Parameters and application areas	Kossel	PKD	EBSD
Crystal orientation mapping and texture analysis			***
Phase discrimination map			++
Pattern quality mapping			+++
Precise lattice constant determination: $\Delta a/a \approx 10^{-5}$	***	++	
Exact determination of crystal orientations: ± 0.05	+++	++	
Crystal structure determination	+++	++	
Symmetry determination, e.g., tetragonal distortion	+++	++	
Detectability, location of crystal defects	+	***	
Estimation of dislocation densities: $10^6 - 10^{10} \text{ cm}^{-2}$ [13, 14]	++	+	
Proof of mechanical tensions and deformations	+++	+	
Determination of the crystal stoichiometry	++	+	
Determination of the expansion coefficient	+++	+	
Determination of the chemical concentration of elements	++		
New formation of phases and phase transformation in the high and low temperature range	++	+	+
Residual stress measurements in micro-range [15-18]	+++	+	
Polar plane distinction at non-centrosymmetric crystals	+++		+
***: main application range; +++: excellent; ++: good; +: possible			

4.1. Precision lattice constant determination by the Kossel technique

The high attainable accuracy for the determination of lattice constants follows from the precise value of the wavelength of the characteristic X-ray of the excited crystal volume of up to $\Delta\lambda/\lambda = 10^{-6}$. According to the material, one uses either K- or L- and M-radiation, respectively, in order to fulfil the Bragg equation. For the lattice constants accuracies in the micro-range of up to $\Delta a/a = 10^{-5}$ arise from that. For these precise values, a high temperature durability during the measurement is required. According to the substance, the exposure times lie at a few minutes. As an example, FeAl (CsCl structure) should be called here, in which a value of $a = (0.29075 \pm 0.00001) \text{ nm}$ which correspond to a relative error of $\Delta a/a = 3 \cdot 10^{-5}$, was determined at the Dresden University of Technology already in the 1960's.

In this substance, tetragonal distortions of the cubic lattice could be found as well, which are expressed by splitting the so-called fivefold intersections (see enlarged detail of Fig. 6 below right), e.g., intersection points of the reflections $(0\ 0\ 2)$, $(1\ 1\ 2)$, $(1\ 0\ 1)$, $(1\ \bar{1}\ 0)$ and $(\bar{1}\ 2\ 1)$. The ascertained distortions are manifested in the ratio $c/a = 1.0045 \pm 0.0006$ [19]. In contrast to today's observation of the interferences by a CCD area detector [20, 21] and subsequent computer evaluation, the original Kossel patterns were detected on X-ray film plates.

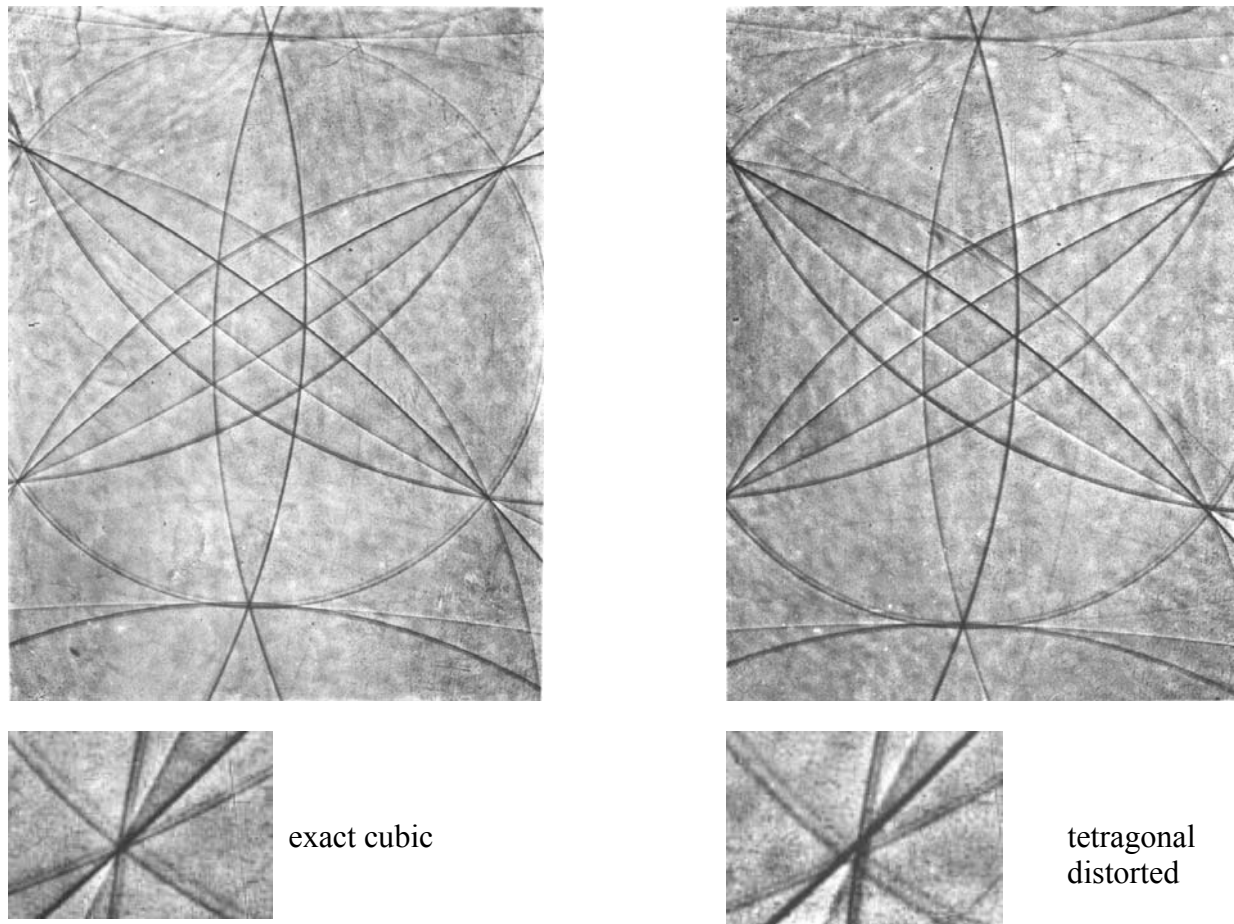


Figure 6. Kossel pattern of FeAl, [110]-pole, with enlarged details below, produced by S. Däbritz (1965) and published in [19, 22].

4.2. Phase transformation of V_3Si at low temperatures

At the intermetallic compound V_3Si (A15-crystal type, transition temperature ≈ 17 K) the lattice transformation tetragonal \Rightarrow cubic was studied in dependence of the temperature. The evaluations of the Kossel pattern in V_3Si specimens deformed plastically at high temperatures provided between 7 and 293 K at low temperatures the in the following Fig. 7 plotted lattice parameter [23].

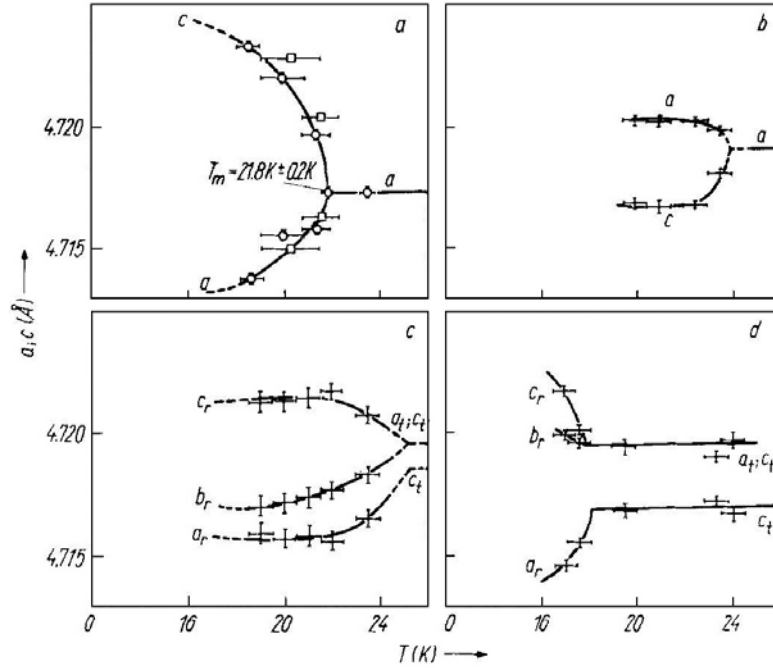


Figure 7. Lattice parameter versus temperature of V_3Si single crystals after plastic deformation; a) two different undeformed samples, i.e., 0 %, b) 8 %, c) 13 %, and d) 12.9 % [23].

4.3. High-temperature Kossel experiments on Cu and phase transformation in Fe

In Table 2, the essential results of high-temperature Kossel investigations attained at the Dresden University of Technology are summarized [24-25]. As marked in the table, lattice constants and thermal expansion coefficients were determined as well as the phase transformations studied extensively. Two examples chosen from the vast amount of investigations will be described in more detail.

a) Phase transformation in Fe

In a single-crystal α -iron (bcc, 99.99 %, dislocation density $< 10^7 \text{ cm}^{-2}$) altogether 16 Kossel patterns were observed up to 1000 °C in steps at intervals of $< 100 \text{ °C}$. It turned out that with increasing temperature both, the contrast and the line sharpness, decrease. From the pattern at 910 °C, the γ -lattice of iron could be proved unambiguously. Clearly, the relationships of the directions of the lattice show the following: the [111]-axis in the [110]-plane of the α -lattice turns into the [110]-axis in the [111]-plane of the γ -lattice:

$$\{110\}_\alpha \parallel \{111\}_\gamma \quad \text{and} \quad \langle 111 \rangle_\alpha \parallel \langle 110 \rangle_\gamma$$

The evaluation of Kossel lines at 1000°C provides the lattice constant value of $a_{1000^\circ\text{C}} = (0.3645 \pm 0.0003) \text{ nm}$ (Fig. 8).

Table 2. Overview of high-temperature Kossel investigations regarding lattice constant changes, and should the occasion arise, phase transformations [24-25].

Material	Temperature range °C	Measurable variable	Relative precision of a-determination
Cu	20 to 800	a	$5 \cdot 10^{-5} - 10^{-4}$
Cu	800 to 1050	a	$4 \cdot 10^{-4}$
Cu	20 to 80	a, α	$3 \cdot 10^{-5}$
Fe	20 to 1000	a, P	$1 \cdot 10^{-4}$
Co	20 to 500	a, c, P	$5 \cdot 10^{-2}$
Ni	20 to 110	a, α	$3 \cdot 10^{-5}$
Fe ₃ O ₄	20 to 850	a, α	$3 \cdot 10^{-4}$
Fe ₃ Al	20 to 100	a, α	$3 \cdot 10^{-5}$
MgCu ₂	20 to 80	a, α	$3 \cdot 10^{-5}$

a, c ... Lattice constant determined

α ... Thermal expansion coefficient ascertained

P ... Phase transformation studied

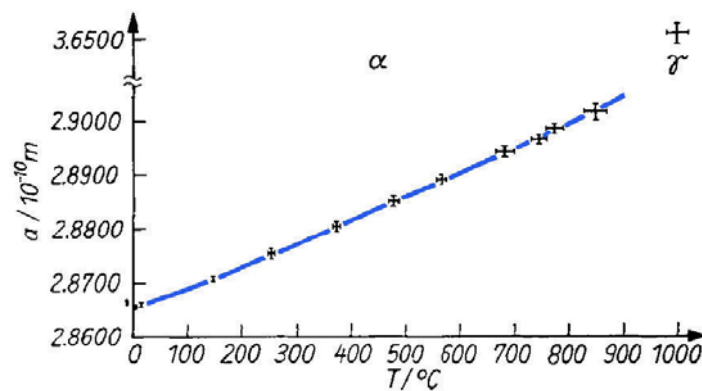


Figure 8. Measured Fe lattice constants versus temperature (α - γ transformation) as well as Kossel pattern of γ -iron at 1000°C: two grains [26].

b) High-temperature experiments on Cu

The high-temperature investigations on copper of up to 1050 °C (melting point: 1083.4 °C) show an interesting connection between the reflection system and the lattice parameter. Without measuring the line distances, in this case the value $a = 0.363111$ nm

($\lambda\text{-Cu-K}\alpha_1 = 0.154055 \text{ nm}$) for the lattice constant, follows immediately with a relative precision of $4 \cdot 10^{-4}$ as at a temperature of $262 \text{ }^\circ\text{C}$ the reflections (042) and (024) touch each other directly (see Fig. 9 left) [24].

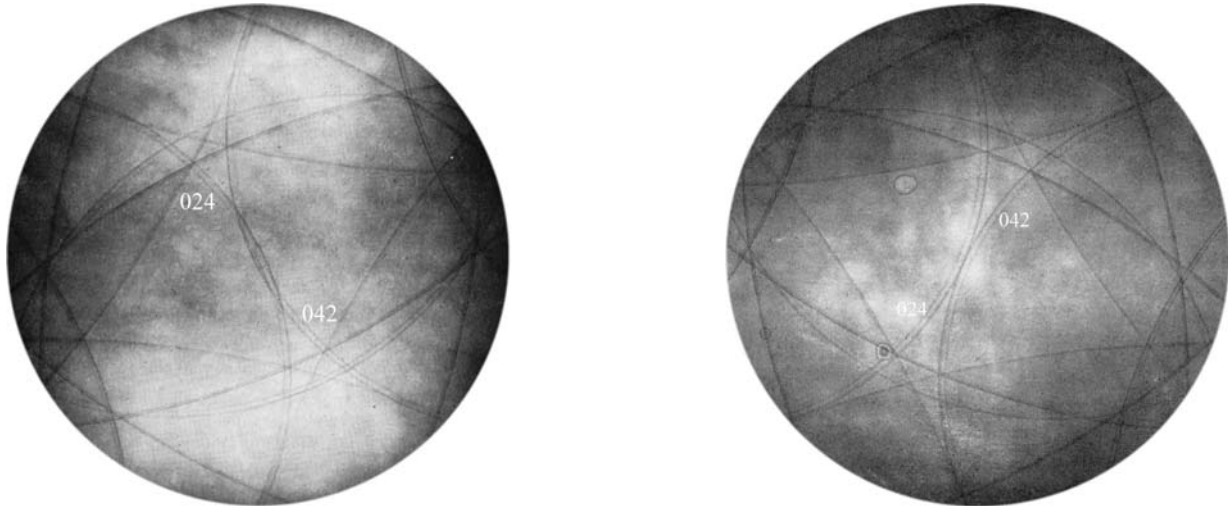


Figure 9. Kossel pattern of Cu at [011]-pole; left at $T = 262 \text{ }^\circ\text{C}$, touch of (042) and (024), right at $T = 363 \text{ }^\circ\text{C}$ (overlapping) [24].

4.4. Characterisation of intermetallic phases in the system Cu-Sn

In model experiments, Cu-Sn/Pb diffusion zones of microelectronic contacts were generated [27], whose intermetallic phases were proved by the Kossel technique for the first time (Fig. 10) [28, 29]. In Table 3, the intermetallic compounds found in the diffusion zones are listed. The phase originally known in the literature as Cu_4Sn could be specified to $\text{Cu}_{41}\text{Sn}_{11}$ with our investigations in the year 1995 already independently of other experiments carried out. With that, the great performance of the Kossel method turned out especially in the characterisation of crystal phases. Fig. 11 shows the simulation belonging to it for each phase.

Table 3. Intermetallic phases in the system Cu-Sn.

Symbol	Phase	Range of existence
ε	Cu_3Sn	room temperature up to $676 \text{ }^\circ\text{C}$
η'	Cu_6Sn_5	room temperature up to $186 \text{ }^\circ\text{C}$
η	Cu_6Sn_5	$186 \text{ }^\circ\text{C}$ to $415 \text{ }^\circ\text{C}$
δ	$\text{Cu}_{41}\text{Sn}_{11}$	$350 \text{ }^\circ\text{C}$ to $586 \text{ }^\circ\text{C}$

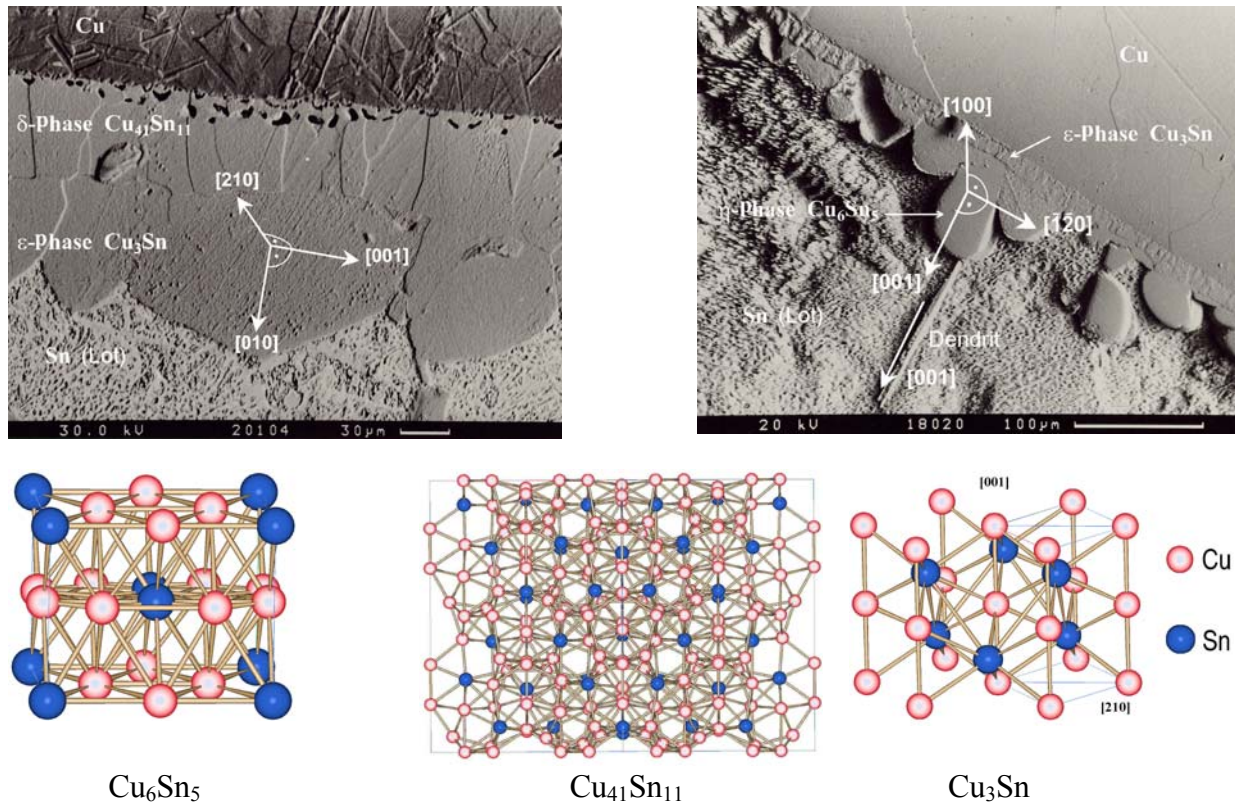


Figure 10. By means of the Kossel technique, determined crystal phases Cu_3Sn , $\text{Cu}_{41}\text{Sn}_{11}$ and Cu_6Sn_5 within the in the corresponding scanning electron micrographs shown diffusion zones [28].

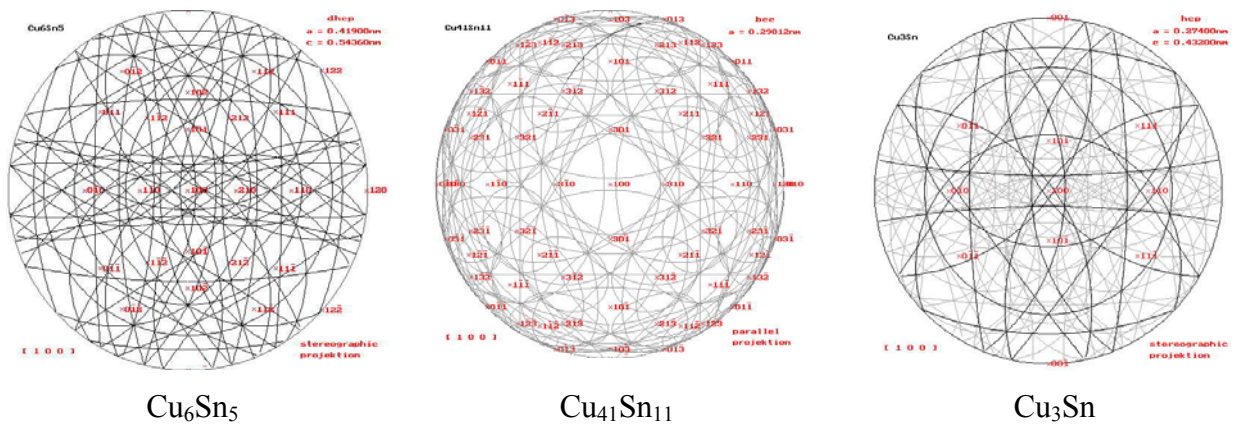


Figure 11. Stereographic projections of the Kossel lines for the three crystal phases [28], which can be calculated with the self-developed simulation program KOPSKO [30].

5. PRESENT AND FUTURE DEVELOPMENTS

5.1. X-ray fluorescence excited Kossel diffraction by polycapillary lenses in SEM

Basic principle of the X-ray fluorescence excited Kossel effect with polycapillary lens in the SEM is shown in Fig. 5 at the beginning. Our preliminary investigations with capillary X-ray optics were carried out using a compact X-ray fluorescence spectrometer [31]. In order to create the possibility of an X-ray excitation of Kossel patterns the X-ray tube IFG iMOXS, with a focusing polycapillary lens, originally intended for fluorescence analysis, was flanged onto a SEM CamScan CS44. The first X-ray fluorescence excited Kossel micro-diffraction patterns in the SEM [32] in transmission is presented in Fig. 12. A large number of mainly Kossel extinction lines are clearly visible. Due to the polychromatic excitation, besides the Kossel reflections, additional Laue reflections may also be observed. The excellent quality of the pattern of Fig. 12 is seen from the noticeable dark-light fine structure at reflections $(1\ 1\ \bar{1})$, $(1\ \bar{1}\ 1)$ and $(\bar{1}\ 1\ 1)$ as well as a field of gradation inside the triangle of the same reflections (marked in Fig. 12 on the right). As a result, the long exposure times of the Kossel pattern excited by an X-ray tube could be decreased to 2 h. It demonstrates how the μ -X-ray fluorescence analysis, the Laue method, and the X-ray excited Kossel diffraction can be combined advantageously with the high lateral resolution of the SEM.

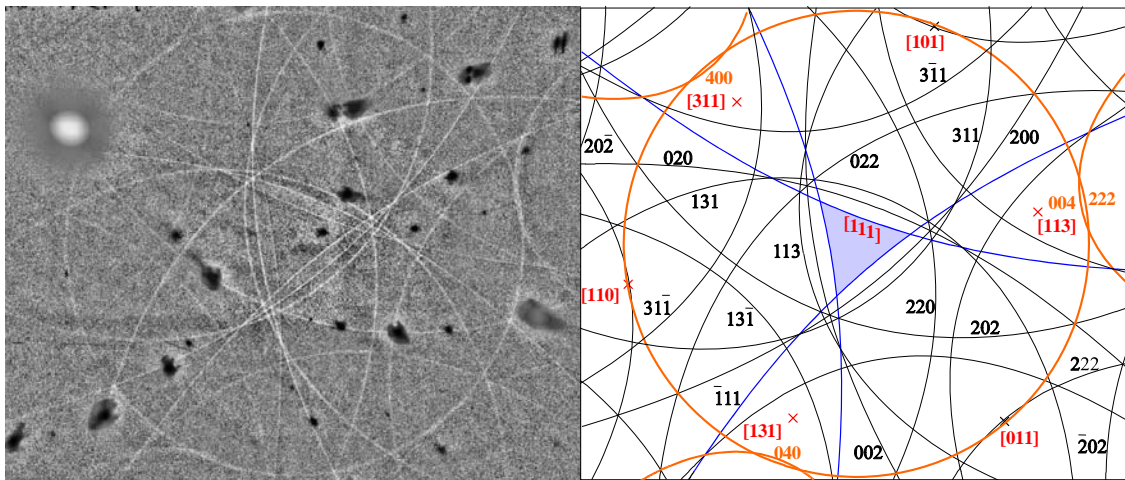


Figure. 12. First X-ray fluorescence excited Kossel micro-diffraction pattern in the SEM, Ni(111)-crystal in transmission with additional Laue-reflections (modified by local contrast compensation) with simulation in gnomonic projection ([111] pole) [32].

5.2. High-resolution residual stress mapping by means of the Kossel technique

For residual stress measurements an extremely high accuracy for the determination of several interplanar crystal spacings is necessary. The high attainable accuracy for the determination of interplanar spacings as partially described in section 4.1 follows from:

- 1) the precise value of the characteristic X-ray wavelength ($\Delta\lambda/\lambda = 10^{-6}$) used;
- 2) the large Bragg angles, i.e. small opening angles of the Kossel cones, and
- 3) the noticeably sharp Kossel diffraction lines, which can be measured precisely.

The first residual stress measurements in the micro-range by means of the Kossel technique using synchrotron excitation were presented by J. Brechbühl, J. Bauch and H.-J. Ullrich in 1996 [15-17]. Fig. 13 shows one of the first examples for a high-resolution residual stress mapping by means of the Kossel technique using electron excitation in the SEM [18]. The distribution of residual stresses of the third kind was determined in the vicinity of a laser cut edge on FeSi₃ electrical sheets [18].

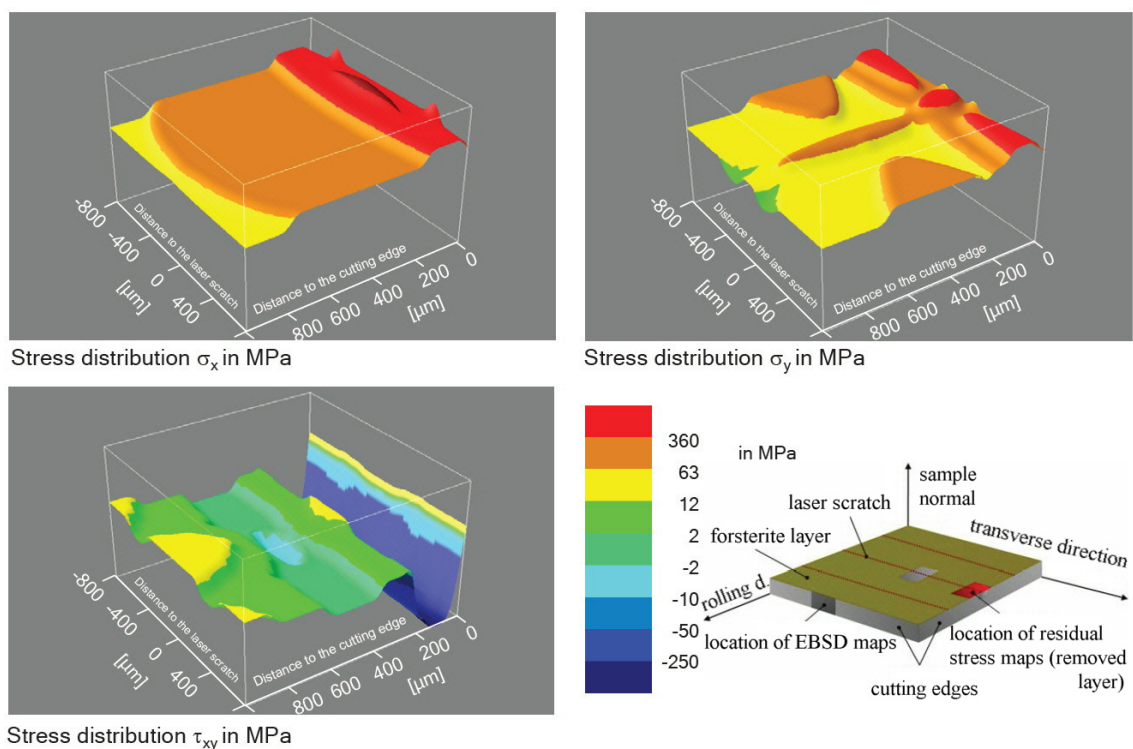


Figure. 13. High-resolution residual stress mapping by means of the Kossel technique showing the distribution of residual stresses in the vicinity of a laser cut edge by M. Böhling and J. Bauch [18] (by courtesy of M. Böhling, Dresden University of Technology).

5.3. Kossel pattern observed by CCD area detector on model samples of deformed Ni

The important advantage nowadays is that the patterns of three different diffraction methods both, X-ray Kossel as well as pseudo-Kossel and the electron backscattered Kikuchi diffraction (EBSD), can be observed by means of only one self-developed scintillator-CCD area detector combination [21, 22] in the SEM. Fig. 14 shows the principles [11] and the corresponding

CCD patterns for each diffraction method in an overview. In each case the patterns of the undeformed Ni crystals are shown on the right side. On the other hand, the observations at 20 % tensile deformed Ni crystals can be seen on the left. By measuring the width of Kossel and pseudo-Kossel reflections, a clear azimuthal dependence of the width of the (111) reflection could be obtained for the 10 % deformed Ni crystals in good agreement with known theoretical models for the line width at dislocation structures formed mainly by *edge dislocations* (Fig. 15) [34].

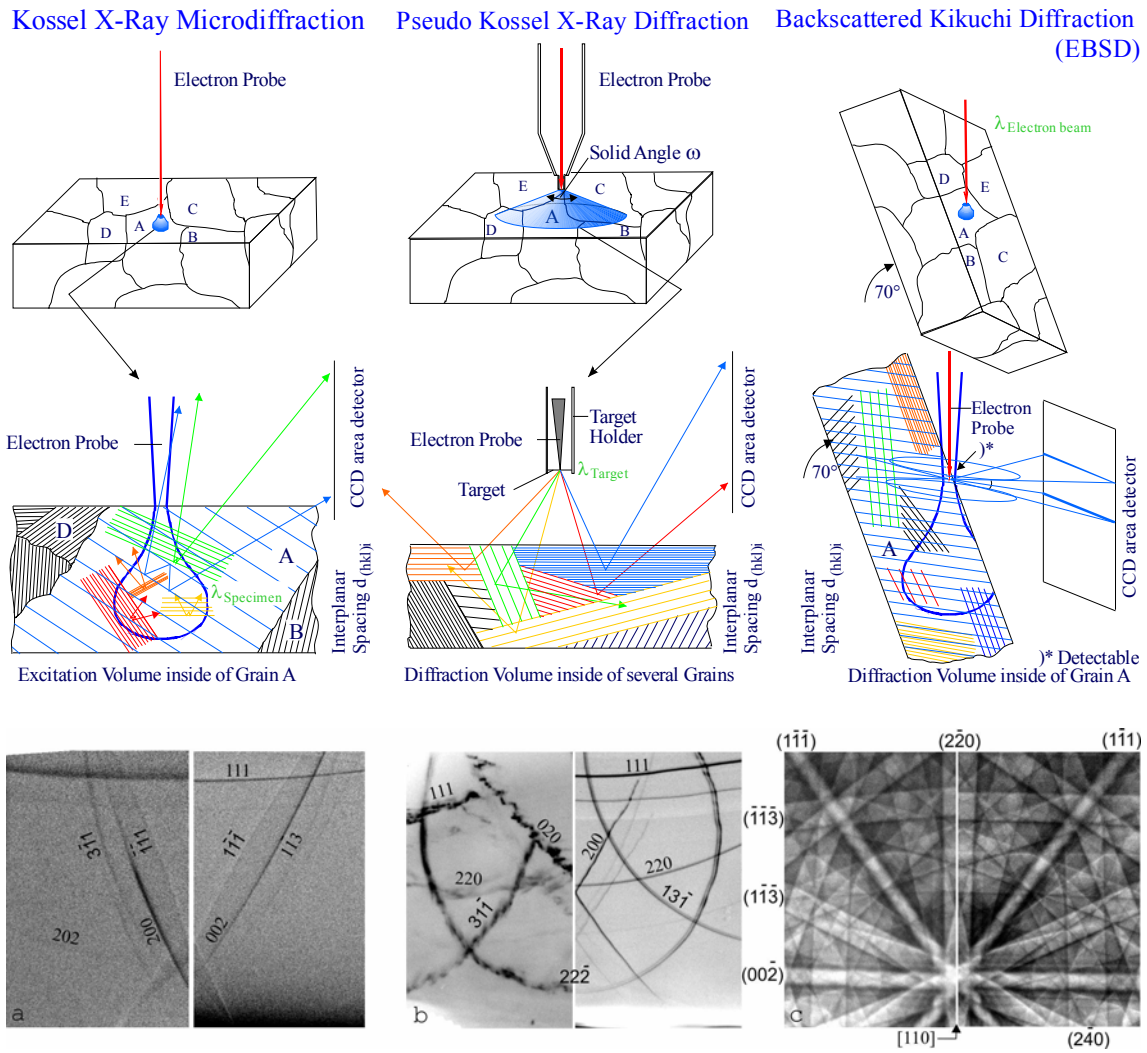


Figure 14. Principles and CCD patterns of X-ray and electron micro diffraction methods in the SEM (on the left half 20 % deformed and on the right half undeformed Ni-crystal).

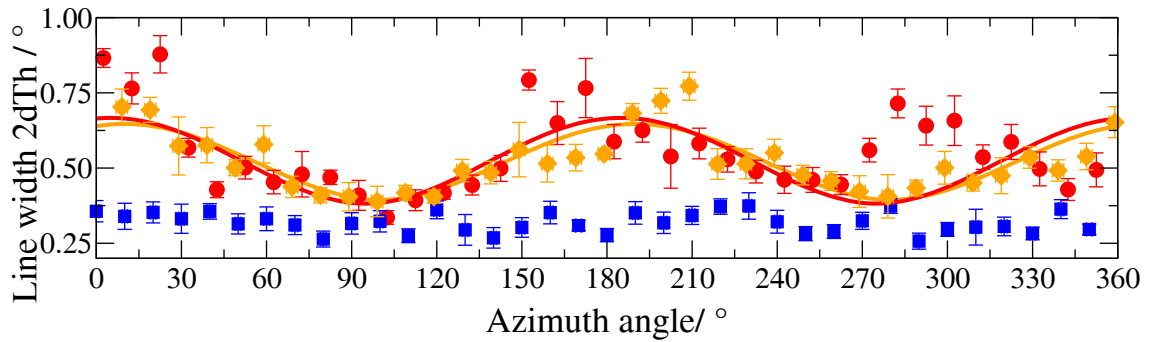


Figure 15. Measured Kossel line width of the (111)-reflection versus the azimuth angle. Comparison between two 10% deformed (●,◆) and undeformed (■) Ni-crystals [34].

5.4. Investigation of crystal defects by the Pseudo-Kossel diffraction in the SEM

The Pseudo-Kossel X-ray diffraction (wide-angle method) is a technique which uses a capillary tube with a thin metal foil (e.g., Fe) near the crystal surface under investigation to form a divergent micro X-ray source by a focused electron beam [35, 36] (Fig. 14, middle). In X-ray pseudo-Kossel patterns information about the crystal structure [37], precise lattice constants, deformation, and stress-strain [38, 39] can be determined non-destructively. However, the influence of crystal defects on this wide-angle pattern have not been sufficiently investigated so far; therefore, one example for a basic investigation shall be presented. Pseudo-Kossel X-ray diffraction patterns of 2 % tensile deformed Ni model crystals were extensively observed in the SEM. As a remarkable irregularity, a lens-shaped splitting of the Fe- $K\alpha_{1/2}$ -(111)-reflection into a principal and a weaker secondary line were found for the first time as shown in Fig. 16 on the left. Kinematic simulations of the line intensity show that a Pseudo-Kossel line splits as described above when crossing a stacking fault (Figs. 16 and 17). Therefore, these characteristic changes of the line profile observed are possibly be caused by this kind of defect. Please compare Fig. 16 on the left with Fig. 17. The basis for these considerations are similar calculations which are known at Kossel-Möllenstedt pattern in the convergent beam electron diffraction in the TEM [40]. Moreover, the origin of the pseudo-Kossel curve section of the fourth order with this irregularity could, in principle, be localized on the crystal surface by simulation and has an extension to the order of 10 μm . There are further investigations necessary in order to confirm these first observations before it can be said that this is a new method for observing stacking faults in the SEM.

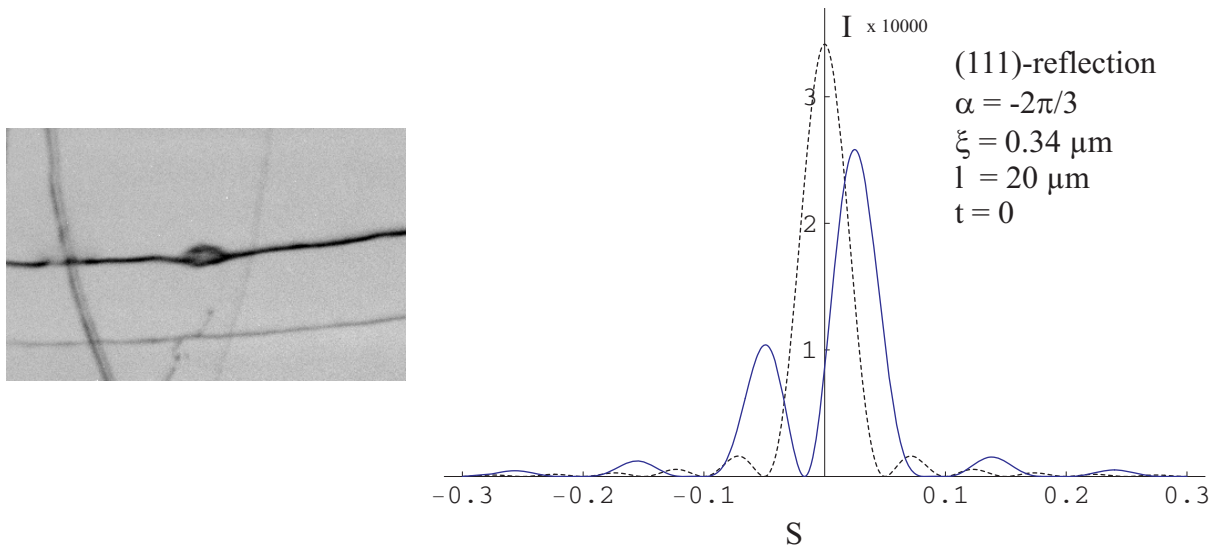


Figure 16. Observed lens-shaped line splitting of the (111) Pseudo-Kossel reflection (left) as well as calculated rocking curve for an ideal crystal (dotted line), and for a crystal with a stacking fault (full line curve), s - Bragg-angle deviation, ξ - primary extinction length, l - absorption depth, t - depth parameter, α - phase shift (right).

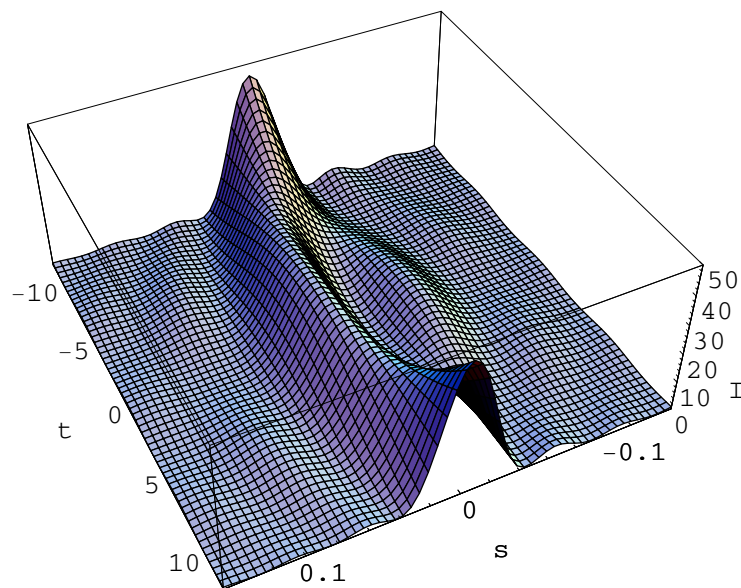


Figure 17. 3 D intensity simulation of the effect of a stacking fault on an X-ray pseudo-Kossel (1 1 1) - reflection for a slightly against the crystal surface tilted stacking disorder perpendicular to this Bragg line (I - intensity: $\times 1000$).

6. REFERENCES

- [1] Borrmann G (1988) *Naturwiss.* **75**, 399.
- [2] Kossel W (1924) *Z. Physik* **23**: 278.
- [3] Kossel W, Loeck V and Voges H (1935) *Z. Physik* **94**: 139.
- [4] Kossel W (1937) *Erg. exakt. Naturwiss.* **16**: 295-352.
- [5] von Laue, M (1960) Röntgenstrahl-Interferenzen. Akad. Verl. Ges.: Frankfurt/Main.
- [6] Borrmann, G (1935) *Naturwiss.* **23**: 591; (1936) *Ann. Phys.* (Leipzig) **27**: 669.
- [7] Geist V and Flaggmeyer R (1974) *Phys. Stat. Sol. (a)* **26**: K1.
- [8] Roberto J B *et al.* (1975) *J. Appl. Phys.* **46**: 936.
- [9] Ullrich H-J, Stephan D, Schmidt D, Kleinstück K and Seeliger D (1975) *Proc 3rd Microprobe Conference*. Berlin, Physical Society of the GDR: 93.
- [10] Ullrich H-J *et al.* (1994) *Nucl. Instrum. Methods Phys. Res. A* **349**: 269.
- [11] Schetelich C, Weber S, Geist V, Schlaubitz M, Ullrich H-J, Kek S and Krane H G (1995) *Nucl. Instrum. Methods. Phys. Res. B* **103**: 236.
- [12] Däbritz S, Langer E and Hauffe W (2001) *Appl. Surf. Sci.* **179**: 38.
- [13] Ullrich H-J *et al.* (1983) *Mikrochim. Acta* **I**: 175.
- [14] Herenz A, Ullrich H-J and Däbritz S (1984) *Proc 6th Microprobe Conference*. Dresden, Physical Society of the GDR: 203.
- [15] Brechbühl J, Bauch J and Ullrich H-J (1999) *Cryst. Res. Technol.* **34**: 59.
- [16] Bauch J *et al.* (1999) *Cryst. Res. Technol.* **34**: 71.
- [17] Bauch J, Wege St, Böhling M and Ullrich H-J (2004) *Cryst. Res. Technol.* **39**: 623.
- [18] Böhling M and Bauch J (2007) *Cryst. Res. Technol.* **42**: 905.
- [19] Ullrich H-J, Thiele K, Däbritz S, Schreiber H, Götze K and Feldhofer F (1972) *Cryst. Res. Technol.* **7**: 1153.
- [20] Däbritz S, Langer E and Hauffe W (1999) *J. Anal. At. Spectrom.* **14**: 409.
- [21] Langer E, Däbritz S, Schurig C and Hauffe W (2001) *Appl. Surf. Sci.* **179**: 45.
- [22] Ullrich H-J and Schulze G E R (1968) *Mikrochim. Acta, Suppl. III*: 188.
- [23] Ullrich H-J, Reinhold U, Däbritz S, Paufler P, Kleinstück K and Pietrass B (1978) *Phys. Stat. Sol. (a)* **49**: 323.
- [24] Ullrich H-J, Däbritz S, Schreiber H (1968) Möllenstedt G and Gaukler K H (eds.): Proc. 5th Intern. Congress on X-Ray Optics and Microanalysis. Tübingen: 406.
- [25] Ullrich H-J (1967) Thesis, University of Technology Dresden.
- [26] Däbritz S (1974) Thesis, University of Technology Dresden.
- [27] Däbritz S, Ullrich H-J and Kleinstück K (1987) *Cryst. Res. Technol.* **22**: 429.
- [28] Däbritz S and Hauffe W (1995) *Fresenius J. Anal. Chem.* **353**: 271.
- [29] Däbritz S, Hauffe W and Kurt R (1997) *Mikrochim. Acta* **125**: 3-12.
- [30] Däbritz S, Langer E and Hauffe W (1997) *Fresenius J. Anal. Chem.* **358**: 148.
- [31] Langer E, Kurt R and Däbritz S (1999) *Cryst. Res. Technol.* **34**: 801-816.
- [32] Langer E, Däbritz S, Hauffe W and Haschke M (2005) *Appl. Surf. Sci.* **252**: 240.
- [33] Langer E, Haschke M and Däbritz S (2008) *Mikrochim. Acta* **161**: 455.

- [34] Langer E, Däbritz S, Schurig C, Breitschneider J and Hieckmann E, unpublished work.
- [35] Langer E, Däbritz S, Kurt R and Hauffe W (1998) *Fresenius J. Anal. Chem.* **361**: 728.
- [36] Langer E *et al.* (1999) *Fresenius J. Anal. Chem.* **365**: 212.
- [37] Bortel G, Tegze M and Faigel G (2005) *J. Appl. Cryst.* **38**: 780.
- [38] Imura T, Weissmann S and Slade J J (1962) *Acta Cryst.* **15**: 786.
- [39] Ellis T *et al.* (1964) *J. Appl. Phys.* **35**: 3364.
- [40] Morniroli J-P (2002) Large-angle convergent-beam electron diffraction (LACBED). Applications to crystal defects. Paris: Société Française des Microscopies.

